FEBS 29151 FEBS Letters 579 (2005) 455–463

PREL1 provides a link from Ras signalling to the actin cytoskeleton via Ena/VASP proteins

Andrea Jenzora[a], Barbara Behrendt[b], J. Victor Small[c], Jürgen Wehland[a], Theresia E.B. Stradal[a,*]

[a] *Department of Cell Biology, German Research Centre for Biotechnology (GBF), 38124 Braunschweig, Germany*
[b] *University Hospital Eppendorf, Institute for Biochemistry and Molecular Biology II (IMB II): Molecular Cell Biology, 20246 Hamburg-Eppendorf, Germany*
[c] *Institute of Molecular Biotechnology (IMBA), Dr. Bohr-Gasse 3-5, 1030 Vienna, Austria*

Received 4 October 2004; revised 18 October 2004; accepted 25 October 2004

Available online 16 December 2004

Edited by Lukas Huber

Abstract **Ena/VASP family proteins are important modulators of cell migration and localize to focal adhesions, stress fibres and the very tips of lamellipodia and filopodia. Proline-rich proteins like vinculin and zyxin are well established interaction partners, which mediate Ena/VASP-recruitment via their EVH1-domains to focal adhesions and stress fibres. However, it is still unclear, which binding partners Ena/VASP proteins may have at lamellipodia tips and how their recruitment to these cellular protrusions is regulated. Here, we report the identification of a novel protein with high similarity to the *C. elegans* MIG-10 protein, which we termed PREL1 (Proline Rich EVH1 Ligand). PREL1 is a 74 kDa protein and shares homology with the Grb7-family of signalling adaptors. We show that PREL1 directly binds to Ena/VASP proteins and co-localizes with them at lamellipodia tips and at focal adhesions in response to Ras activation. Moreover, PREL1 directly binds to activated Ras in a phosphoinositide-dependent manner. Thus, our data pinpoint PREL1 as the first direct link between Ras signalling and cytoskeletal remodelling via Ena/VASP proteins during cell migration and spreading.**

Keywords: Ras; VASP; Mena; Actin; Lamellipodium; Focal adhesion

1. Introduction

The actin cytoskeleton is a prerequisite for cell motility and undergoes various rearrangements during lamellipodia and filopodia formation, bundling into stress fibres or anchorage to the substrate through focal adhesions. Cell migration is mediated by a concerted interplay of assembly and disassembly of all these structures, the formation of which is tightly regulated by small GTPases of the Rho family [1,2]. The protrusion of lamellipodia and filopodia requires actin polymerization involving the de novo nucleation of actin filaments and the addition of monomers to the barbed ends of pre-existing filaments [3,4]. Incorporation of actin into dynamic structures is restricted to the sites, e.g., the lamellipodial tip [5], where the fast growing (barbed) ends of the filaments are located [6]. There is accumulating evidence for the presence of multi protein-complexes at the very edges or tips of protruding lamellipodia and filopodia harbouring components directly driving actin nucleation via the Arp2/3 complex [7,8], and other factors exerting modulatory functions [9, reviewed in 10,11,12].

Bar-Sagi and Feramisco showed already in 1986 [13] that injection of constitutively active Ras into fibroblasts induces membrane ruffling, providing a first link between Ras signalling and the actin cytoskeleton. The ability of active Ras to increase the invasive potential and motility of fibroblastic cells was proposed to be mediated by the suppression of integrin activation and adhesion [14, reviewed in 15]. On the contrary, the Ras family member Rap1 was found to reverse the phenotype of Ras transformation, to induce adhesion and to trigger integrin activation in response to its activation [16, reviewed in 17].

In addition to the inside out signalling effects of Ras on integrin activation, engagement of integrins, e.g., through binding to fibronectin, leads to Ras- and subsequent Erk activation, which coincides with transient association of Ras with the sites of integrin engagement [2,18]. Moreover, Nobes and Hall showed that Ras- but not Erk activation is required for the onset of cell migration in wound healing assays, as exemplified by microinjection of neutralizing anti-Ras antibodies and chemical inhibitors of MEK [2]. Nevertheless, the molecular link from Ras to actin reorganization and adhesion turnover during cell motility is poorly defined.

Ena/VASP proteins are important regulators of the actin polymerization machinery, although the exact mechanism of how this regulation occurs is under debate [12,19]. They are localized to focal adhesions, along stress fibres and at the tips of protruding lamellipodia and filopodia [9,20–22] and are binding partners of the actin monomer binding protein profilin [21,23]. Combined genetic inactivation of the Ena/VASP family members VASP and Mena indicated that these proteins may not be essential for the formation of lamellipodia and filopodia, although fibroblasts lacking these family members display alterations in migratory behaviour and protrusion efficiency [11,12]. Actin-based motility of the facultative intracellular pathogen *Listeria monocytogenes* is enhanced by Ena/VASP proteins, both in vivo [24] and in vitro [25]. Ena/VASP proteins interact directly with the *Listeria* surface protein ActA and the enhanced motility was attributed to the recruitment of profilactin by VASP [23,26] to promote localized actin assembly [27]. However, in vitro, Ena/VASP proteins can also enhance actin based motility in the absence of profilin [19].

The surface protein ActA of *Listeria* is essential and sufficient for the intra- and inter-cellular actin-based motility of this pathogen. A poly-proline motif flanked by hydrophobic

*Corresponding author. Fax: +49 531 6181 444.
E-mail address: ths@gbf.de (T.E.B. Stradal).

0014-5793/$22.00
doi:10.1016/j.febslet.2004.10.110

and acidic residues was identified to mediate recruitment of Ena/VASP proteins by binding to their N-terminal EVH1 domains [28]. Moreover, homologous polyproline repeats in zyxin [29] and vinculin [30] were shown to be involved in the targeting of Ena/VASP proteins, via their EVH1 domains, to focal adhesions.

Additional proteins harbouring EVH1-binding motifs were identified more recently, for instance the haematopoietic protein Fyb/Slap/ADAP, which binds to Ena/VASP family proteins upon T-cell receptor activation [31], and palladin, also implicated in contributing to subcellular Ena/VASP positioning [32]. However, it remained unclear as to which interaction partners Ena/VASP proteins may have at lamellipodia tips and how they are recruited to this subcellular compartment. Recently, for instance, the proto-cadherin Fat1 was found to be capable of interacting with Ena/VASP proteins at these sites, providing a potential mechanism for Ena/VASP recruitment to lamellipodia [33].

The starting point of the present study was our finding that a monoclonal antibody raised against zyxin recognized the repeated EVH1-binding consensus (D/E-FPPPP-XD/E) in both zyxin and vinculin, and stained lamellipodia tips in migrating fibroblasts, sites lacking both zyxin and vinculin [34]. Using this antibody, we identified a novel protein from a HeLa expression library with high similarity to the *C. elegans* MIG-10 protein [35,36], which we have tentatively termed PREL 1 for **P**roline-**R**ich **E**VH1 **L**igand 1.

MIG-10 is a 73 kDa protein and shares sequence homology with the Grb7-family of signalling adaptors [36–38]. Unlike the GRB7/10/14 sub-family, MIG-10 and the novel protein identified in this study lack the C-terminal src homology 2 (SH2) domain and harbour multiple poly-proline stretches. We found that PREL 1 not only binds to VASP and Mena and co-localizes with these proteins at lamellipodia tips and in focal adhesions, but that it also interacts with GTP-loaded Ras in a lipid dependent manner. These findings thus provide a direct link between Ras signalling and remodelling of the actin cytoskeleton via Ena/VASP proteins.

2. Materials and methods

2.1. Cells and transfections

All tissue culture reagents were from Gibco BRL and all chemicals were from Sigma unless mentioned otherwise. B16F1 (ATCC: CRL-6323) cells were maintained as described earlier [39]. Rat2 cells (ATCC: CRL-1764) were cultured in DMEM supplemented with 10% FCS (PAA Gold) and 2 mM glutamine. Swiss 3T3 (ATCC: CCL-92) and NIH3T3 cells (ATCC: CRL-1658) were cultured in DMEM supplemented with 10% FBS (Sigma), 2 mM glutamine 1.5% non-essential aminoacids and 1% Na-pyruvate. Transfections were carried out with SuperFect (Quiagen, Germany, for B16-F1) or with FuGENE (Roche, Germany, for Rat2 and NIH 3T3), according to the manufacturer's protocols.

2.2. Identification of PREL1 and cloning of expression constructs

Screening of a HeLa cell expression library (#69656-3; Novagen Inc., Madison) was carried out as described earlier [31] using the monoclonal antibody 31C4 (isotype IgM), which recognizes the EVH1-recognition consensus, leading to the identification of a novel open reading frame (ORF) with high similarity to the murine ORF prp48 (Acc. No.: AF020313) and the nematode *mig-10* sequence. Reverse transcription (RT)-PCR was carried out to obtain the full length sequence information using the Titan Kit (Roche) according to the manufacturer's instructions. Human brain total RNA was used as a template and was obtained from Ambion (Huston, TX). The expressed sequence tag (EST) clone (Acc. No.: 14500382) was obtained from the Resource Centre of the German Human Genome Project (RZPD, Berlin, Germany) and contained the full length coding sequence of the murine gene.

Murine full length PREL1 derived from the above EST clone was sub-cloned into pEGFP-C or pEGFP-N vectors (Clontech, Palo Alto, CA). Constructs encoding the proline-rich N-terminus (residues 1–252) and C-terminus (residues 398–668), the RA-domain (residues 151–276) and the PH-domain (residues 301–433) were generated by PCR and cloned into pEGFP-C (Clontech) and pGEX-6P (Amersham) vectors for eucaryotic and bacterial expression, respectively. All sequences were confirmed by sequencing. An overview of the constructs used in this study is available in the Supplementary Information.

2.3. Antibodies

The monoclonal antibody (subtype IgM, clone 31C4) recognizing the poly-proline region of zyxin was generated against recombinant human full length zyxin [34]. Epitope mapping was performed as described earlier [40].

Polyclonal rabbit antiserum termed pcVASP1 was raised against the synthetic peptide: C-ATQVGEKPPKDESASQEESEARLPAQ derived from the murine VASP sequence. The anti-PREL1 antiserum pcPREL1 was raised against a bacterially expressed GST-tagged fragment of PREL1 comprising residues 1–420. Antisera were affinity purified using the respective peptides or recombinant proteins immobilized on CNBr-sepharose 4B (Amersham Biosciences, Sweden). Specificity of the antisera was confirmed by Western blot detection of the endogenous and ectopically expressed GFP-tagged proteins. Monoclonal anti-Mena antibody was described earlier [21]. Antibodies specific for GFP and Zyxin [34] were from Synaptic Systems (Göttingen, Germany). Monoclonal anti-GST antibody was raised using recombinant GST as an antigen and characterized as described [40]. Monoclonal anti-vinculin antibody was from Sigma (Munich, Germany), the monoclonal anti-Ras antibody was from Upstate Biotechnology (Charlottsville, VA), and the anti-myc antibody was purchased from Abcam (Cambridge, UK).

2.4. Immunofluorescence, video microscopy, and data processing

Cells were plated on glass coverslips coated with either 25 μg/ml laminin (Sigma) or 50 μg/ml fibronectin (Roche) prior to either fixation or video microscopy as indicated. Immunofluorescence staining was performed essentially as described [41]. Secondary reagents were Alexa Fluor®488- or Alexa Fluor®594-coupled goat antibodies, which were used in combination with or without Alexa Fluor-dye coupled phalloidins (Molecular Probes, Leiden, The Netherlands) to label the actin cytoskeleton.

Video microscopy and microinjection of live B16-F1 and NIH3T3 cells expressing GFP-tagged variants of PREL1 were performed as described earlier [9]. V12Ras was purified as described [42] and injected at 2.5 mg/ml in a mixture with 0.25 mg/ml Texas-Red-labelled dextrane (70 kDa, Molecular Probes) to control for successful injections. TPA (tetradecanoyl phorbol acetate)-treatments were performed at a concentration of 1 μg/ml.

Data were acquired using a Zeiss Axiovert 135TV microscope equipped with a back-illuminated cooled charge-coupled device camera (Princeton Research Instruments) driven by IPLab software (Scanalytics, Fairfax, VA) and processed using IPLab and Adobe Photoshop 6.0 (Adobe Systems, San Jose, CA) software. Statistical analyses were carried out using Microsoft Excel 2001 and Sigma Plot 8 software.

2.5. Immunoprecipitations and pull-down assays

For immunoprecipitations, cells grown in 10 cm diameter dishes were washed with PBS and lysed in 500 μl of ice-cold lysis buffer L1 (8 mM Tris base, 12 mM HEPES, 50 mM NaCl, 15 mM KCl, 12 mM $MgCl_2$, 1 mM EGTA, 20 mM NaF, 1 mM Na_3VO_4, 1% PEG 6000, and Complete Mini™, EDTA-free protease inhibitor cocktail (Roche) supplemented with or without 1% Triton X-100 as indicated) for 10 min on ice. In the absence of detergents, cells were harvested with a cell scraper and lysed by three 10 s pulses in an ultrasonic water bath (RK 102H, Bandelin electronic, Berlin, Germany) with 5 s vortexing steps in between. All lysates were cleared by centrifugation for 15 min at 12 000 × *g* and 4 °C. Cleared lysates were incubated with

5 μg of the indicated antibodies for 1 h and followed by incubation with 30 μl protein G-sepharose beads (Amersham Biosciences) under agitation for 45 min at 4 °C. Beads were then washed twice with lysis buffer. Precipitates were resolved by SDS–PAGE and analysed by immunoblotting.

For pull-down assays, the recombinant GST-tagged proteins or recombinant GST alone as control (for constructs, see Supplementary Material) were coupled to glutathione-sepharose beads (Pharmacia) and washed in buffer B (50 mM Tris, pH 7.5, 50 mM NaCl, 5 mM $MgCl_2$, and 0.1 mM DTT). Final concentration of the recombinant protein on beads was 2 mg/ml slurry. 30 μl of beads was incubated with cleared lysates (see above) for 1 h at 4 °C, washed twice with lysis-buffer and resuspended in SDS-loading buffer. Precipitates were resolved by SDS–PAGE and analysed by immunoblotting. For precipitations of endogenous Mena in Fig. 3(a) and (c), Rat-2 cells were used instead of NIH3T3 due to the high expression levels of this protein as compared to the latter cell line.

2.6. Protein overlay assays on immobilized peptides and lipids

0.2 mg/ml purified recombinant EVH1-domains of Mena, VASP and Evl fused to GST [28,43] were incubated on peptide-scans comprising either the proline-rich N- or C-terminus of murine PREL1 in TBS-T containing 10% FCS as described earlier [28]. Detection was performed in analogy to Western blot membranes using a monoclonal anti GST antibody. For protein-lipid overlays, 0.01 μg/ml of the purified recombinant GST-tagged PH-domain of PREL1 was incubated on PIP-strips (Echelon Research Inc.) and developed as described above. Binding of the GST-tagged EVH1- and PH domains in overlays was quantified by luminometry employing a cooled CCD-camera (Fuji) and analysed using AIDA software (Raytest, Germany). Signals from areas of identical size were integrated, background subtracted and normalized to 100 as a value for the highest binding.

2.7. Spreading assay and Ras activation assay

10E4 NIH3T3 cells were plated on fibronectin (50 μg/ml, Roche) coated glass coverslips (12 mm diameter) in 24 well plates and fixed with 4% PFA/PBS after different time points as indicated. Cells were permeabilized with 0.1% TX-100 in 4% PFA for 45 s, washed with PBS and stained with the polyclonal anti PREL1 antibody as described above. At 10, 20, 40 or 60 min after plating, the number of cells that had already initiated spreading was quantified. In addition, the fraction of spreading cells was scored for PREL1 localization at lamellipodia tips for each timepoint ($n \geqslant 300$). In parallel, 2x10E6 NIH3T3 cells were plated on fibronectin coated (20 μg/ml, Roche) 10 cm diameter dishes and subjected to Ras activation assays after different time points according to the manufacturer's instructions (Upstate Biotechnology). Levels of GTP-Ras were assessed by luminometry employing a cooled CCD-camera (Fuji) and analysed using AIDA software (Raytest, Germany).

3. Results and discussion

3.1. Identification of PREL1

When characterizing monoclonal antibodies raised against human recombinant zyxin [34], a clone was identified (see also Section 2), which not only recognized zyxin, but also vinculin and a number of unidentified bands in Western blots of lysates of various cell lines (Fig. 1(a)). In immunofluorescence, this antibody stained focal adhesions and stress fibres of fibroblastic cells, where zyxin and vinculin are enriched, as well as the tips of protruding lamellipodia (Fig. 1(b)).

In order to identify novel ligands for Ena/VASP proteins, we screened a HeLa expression library employing the above antibody. From this screen, we derived several crossreactive clones, which were identified as the Rho-GEF LARG (Acc. No.: NP_056128), the ERM family member Radixin (Acc. No.: NP_002897) and a novel protein, with sequence similarity to the murine ORF prp48 (Acc. No.: AF020313), which was identified earlier (together with Mena) in a screen for potential binding partners of the WW domain of FE65 (PRP48 for Proline Rich Protein from clone number 48) [44]. We tentatively termed this novel protein PREL1 (**P**roline **R**ich **E**VH1 **L**igand 1).

Sequence analyses and database searches revealed that the human and the murine sequences of PREL1 comprise a coding sequence of 1998 and 2007 base pairs, respectively, encoding a protein with numerous proline-rich stretches in their N- and C-termini and a calculated molecular mass of 73 and 74 kDa, respectively. In addition, the protein displays a Ras association (RA) and a pleckstrin homology (PH) domain, both of which are embedded in a stretch of residues that shows homology to and defines the Grb7/10/14 family of signalling adaptors [36] (Fig. 1(c)). This region of sequence-homology of approximately 300 amino-acid residues was also identified in the *C. elegans* protein MIG-10 and was termed the GM-region (Grb7-MIG-10 homology region) [36,38]. MIG-10, the putative *C. elegans* ortholog of PREL1, has been implicated in neuronal cell migration during embryonic development of the nematode [35,45].

Two homologous genes are present in mammals, PREL1 identified here and the open reading frame KIAA1681 (which we tentatively named PREL2) with calculated molecular weights of 74 and 134 kDa, respectively. PREL1 and PREL2 (KIAA1681) show a high degree of sequence homology also outside the GM region especially in the N-terminus, while the most striking difference between them is the size of the C-terminal proline-rich extension. (For a detailed alignment see Supplementary Material.)

The *C. elegans* genome harbours one PREL-like gene, i.e., MIG-10, with significant homology to PREL1, while the only PREL-like gene detectable in the genomes of *Drosophila melanogaster* (CG11940) and *Anopheles gambia* (agCP1621) display higher homology to PREL2. Thus, these two novel proteins, mammalian PREL1 and PREL2, may constitute a new protein family together with MIG-10 and the gene products encoded by the fly database entries.

Interestingly, PREL2 (KIAA1681) is located on a region of human chromosome 10, which has been implicated in the inherited neuro-degenerative disease Amylotrophic Lateral Sclerosis 2 (ALS2) and was therefore discussed as a potential candidate (ALS2 candidate region 9: ALS2CR9) involved in the development of this disease [46].

3.2. Expression pattern, localization and dynamics of PREL1

To learn more about the expression pattern, tissue distribution and sub-cellular localization of PREL1, we raised polyclonal antibodies against recombinant fragments or synthetic peptides derived from different regions within the protein. One antiserum characterized in more detail specifically recognized endogenous PREL1, ectopically expressed GFP-tagged PREL1 as well as the recombinant protein and revealed an apparent molecular weight of PREL1 of 100 kDa on Western blots (Fig. 2(a)). Western blot analyses of different cultured cell lines and various mouse tissues (Fig. 2(b)) using the novel polyclonal antiserum showed that PREL1 is widely expressed and enriched in the haematopoietic system.

Immunolabelling experiments using affinity purified polyclonal anti-PREL1 antibodies revealed a strong signal at lamellipodial tips and in addition at focal adhesions in Swiss 3T3 fibroblasts growing on fibronectin (Fig. 2(c)). To further con-

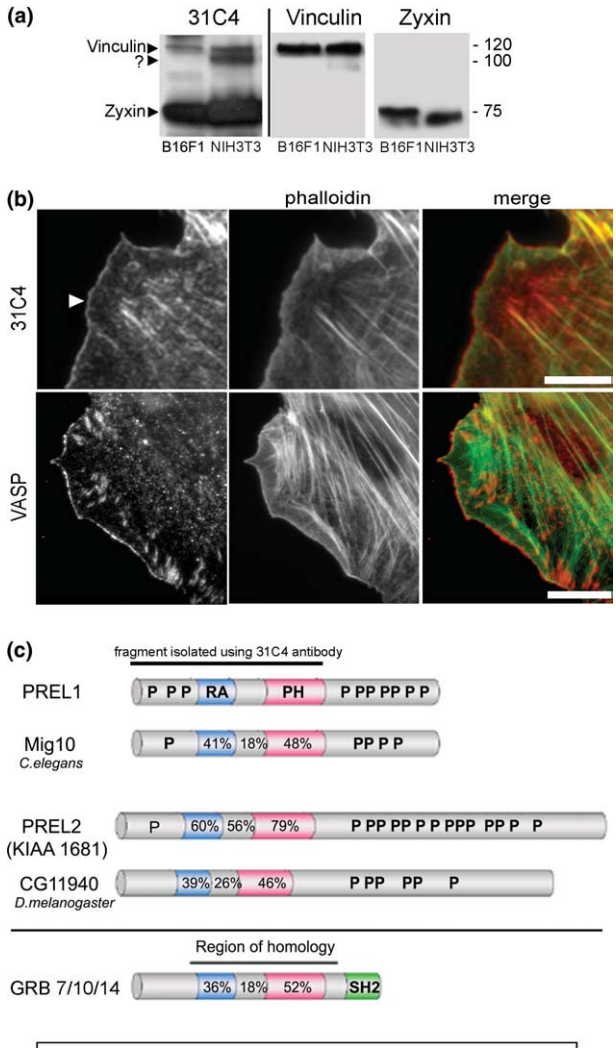

Fig. 1. PREL1 is a novel proline rich protein. (a) Identification of a novel proline rich protein with an apparent molecular weight of 100 kDa in lysates of murine NIH3T3 fibroblasts employing a monoclonal antibody (31C4, subtype IgM) that recognizes the EVH1-recognition motifs in zyxin and vinculin. Detection of zyxin (75 kDa) and vinculin (120 kDa) was confirmed employing specific antibodies, respectively, as indicated. Note that endogenous PREL1 is not detectable in lysates of murine B16-F1 melanoma cells. (b) In Swiss 3T3 fibroblasts growing on fibronectin, the 31C4 antibody stained both focal adhesions and the very edge of lamellipodia (arrowhead), as confirmed by counterstaining of the actin cytoskeleton with phalloidin. This distribution is highly reminiscent of the localization pattern of Ena/VASP family proteins as exemplified by labelling with polyclonal anti-VASP antibodies (pcVASP). Scale bars equal 20 μm. (c) Domain overview of the newly identified PREL1 as compared to the *C. elegans* MIG-10 protein, the open reading frame KIAA1681 (PREL2), an uncharacterized *Drosophila* open reading frame (CG11940) as well as the Grb7/10/14 family. The top line marks the fragment of PREL1 that was isolated from a HeLa expression library in the 31C4 screen. The percentages display the degree of sequence identity within the domains of the depicted proteins and P indicates the location of poly-proline stretches. All proteins share a central RA (Ras association) and PH (pleckstrin homology) domain embedded in a larger region of homology termed GM region, for Grb7/10/14 and MIG-10 region of homology.

firm this localization, we fused the murine full length cDNA to EGFP (either N- or C-terminally) and visualized its dynamics in B16-F1 cells moving on laminin. These studies confirmed that PREL1 can indeed be recruited to the tips of lamellipodia (Fig. 2(d)) reminiscent of the distribution of VASP during lamellipodia protrusion [9] and, less prominently, to focal adhesions (Fig. 2(d)). Notably however, while PREL1 robustly targeted to the tips of protruding lamellipodia in B16-F1 and Swiss 3T3 cells, video microscopy of GFP-PREL1 in NIH3T3 cells (not shown) or immunolabelling of endogenous PREL1 in the same cells revealed a more complex distribution pattern, since lamellipodia protrusion was not always coincident with PREL1 recruitment to their tips. Therefore, we conclude that PREL1 is targeted to focal adhesions and lamellipodia in a cell type and/or signalling status-specific manner (see also Figs. 5 and 6).

3.3. Interaction of PREL1 with Ena/VASP proteins via N-terminal and C-terminal poly-proline motifs

To test for a direct interaction of PREL1 with Ena/VASP proteins, we performed co-immunoprecipitation experiments using monoclonal anti-Mena and polyclonal anti-PREL1 antibodies. In these experiments, the Ena/VASP family protein Mena co-precipitated moderate amounts of ectopically expressed untagged PREL1 and anti-PREL1 antibodies co-precipitated endogenous Mena from the same lysates, suggesting that at least a sub-portion of Mena and PREL1 is bound to each other in vivo (Fig. 3(a)). Analogous experiments were performed to analyse the interaction of endogenous PREL1 and the Ena/VASP-family member VASP in NIH 3T3 cells with virtually identical results (not shown).

To assess whether the interaction was direct and whether an EVH1 domain/poly-proline interaction accounts for the binding of PREL1 to Mena and VASP as predicted from the sequence of PREL1, we performed pull-down assays with GST-tagged EVH1 domains from lysates of cells expressing different GFP-tagged constructs comprising either the N-terminal or C-terminal proline-rich motifs of PREL1. In these pull-down assays, significant amounts of both the N-terminus and the C-terminus of PREL1 as well as the endogenous full length protein or the ectopically expressed protein fused to GFP could be precipitated from cellular lysates (Fig. 3(b)). In addition, we performed pull-down assays using the recombinant GST-tagged proline-rich N- and C-terminus of PREL1. Endogenous Mena and VASP were readily coprecipitated from lysates of Rat-2 and NIH3T3 cells, respectively (Fig. 3(c)).

To further identify those poly-proline motifs of PREL1 that mediate direct binding to the EVH1 domains of Ena/VASP family proteins, we employed the peptide overlay technique [28] (Fig. 3(e) and (f)). The proline rich sequences of the N-terminus (residues 1–160) as well as the C-terminus (residues 433–668) of PREL1 were synthesized in an immobilized form on a membrane as an array of 15-mer peptides with an overlap of 12 AA with the preceding and the subsequent peptides, respectively [28,47].

Under these conditions, two of the proline rich stretches, one in the N-terminus (Fig. 3(e)) and one in the C-terminus (Fig. 3(f)), displayed significant binding to GST-tagged recombinant EVH1 domains of Mena (Fig. 3(e) and (f)), VASP and EVL (not shown). In vitro binding of the recombinant EVH1 domains to the other proline rich motifs was significantly weaker as compared to the motifs highlighted in Fig. 3(e) and (f). In addition, binding to the N-terminal motif was app. 1.5-fold lower as compared to the C-terminal motif (for signal quantification, see Section 2). This latter motif also displays the highest degree of conservation to the EVH1 binding consensus motif D/EFPPPPXD/E [28].

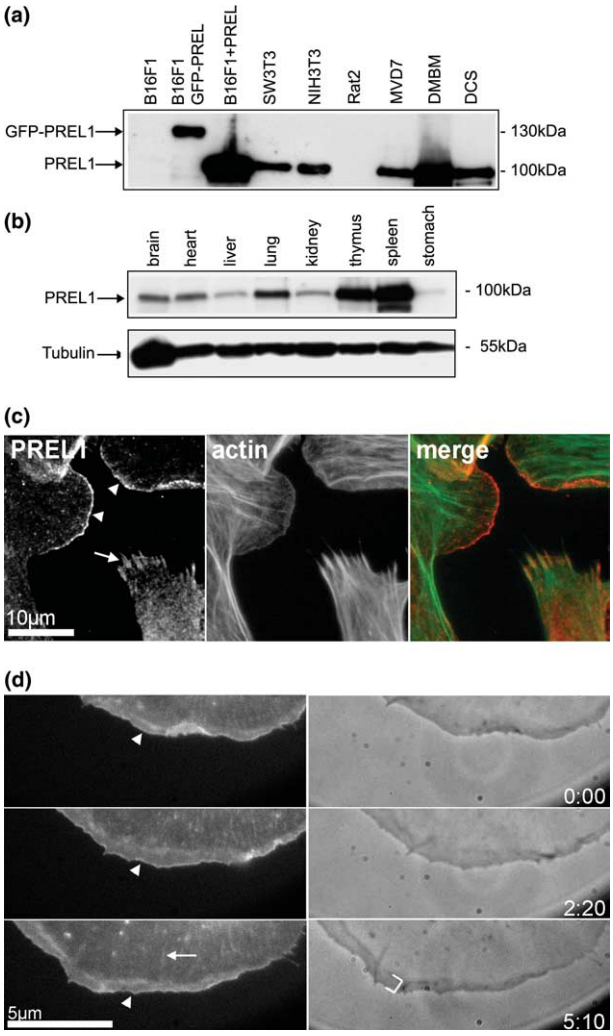

Fig. 2. Expression pattern and subcellular distribution of PREL1. (a,b) Western blotting of PREL1 from extracts of different cultured cell lines (a) and various mouse tissues (b) revealed that PREL1 is widely expressed and highly enriched in tissues or cells of haematopoietic origin. (DMBM: bone marrow macrophages, DCS: dendritic cells). Tubulin detection was used as loading control. Note that GFP-tagged and untagged PREL1 are readily expressed in B16F1 cells lacking the endogenous protein. A Western blot loaded with various samples and showing the whole molecular weight range can be viewed in the Supplementary Material. (c) Swiss3T3 cells were immunolabelled with polyclonal anti-PREL1 antibodies (pcPREL1) and counterstained for filamentous actin with phalloidin as indicated. In these cells, PREL1 is localized at the very edge of lamellipodia (arrowhead) and in focal adhesions (arrow). Scale bar equals 10 µm. (d) Time lapse phase contrast (right panels) and fluorescence (left) microscopy of B16-F1 mouse melanoma cells transfected with EGFP-tagged PREL1 moving on laminin. The panels display representative frames at three consecutive timepoints during protrusion of the cell front. Time is given in minutes and seconds. Note the recruitment of GFP-tagged PREL1 to the lamellipodium tip (arrowheads) and less prominently to focal adhesions (arrow). The bracket in the bottom phase contrast image marks the width of the lamellipodium. Scale bar equals 5 µm.

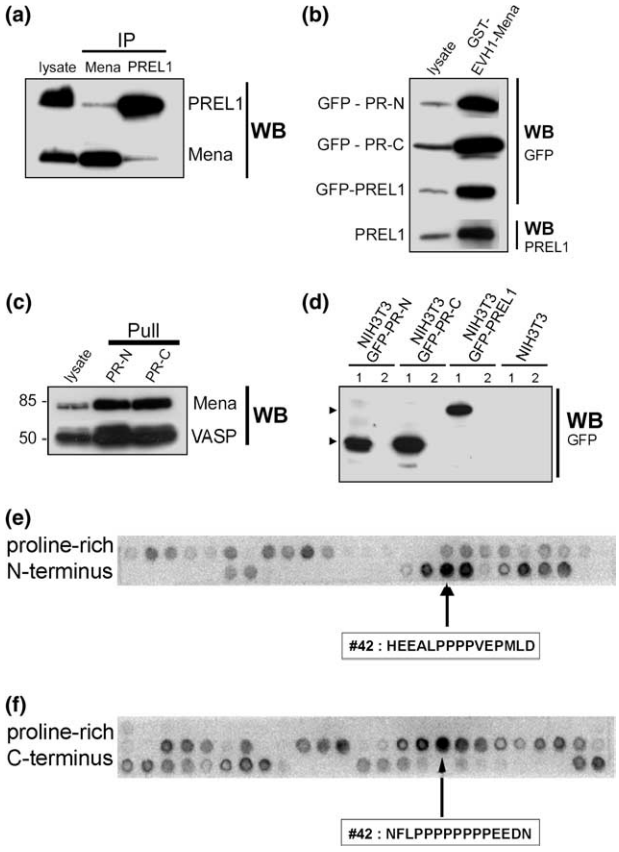

Fig. 3. PREL1 binds to the EVH1 domains of Ena/VASP proteins in vivo and in vitro. (a) Co-immunoprecipitations of PREL1 and Mena using either the polyclonal anti PREL1 antibody pcPREL1 or a monoclonal anti Mena antibody [21]. (b) Pull-down experiments with the GST-tagged EVH1 domain of Mena from lysates of NIH3T3 cells expressing the GFP-tagged proline-rich N- (PR-N) and C-termini (PR-C) or GFP-tagged full length PREL1. The EVH1 domain readily precipitated both the N- and C-terminal proline-rich domains of PREL1 as well as the endogenous and the GFP-tagged full length protein. Western blot detection was performed using either a monoclonal anti-GFP antibody or polyclonal anti-PREL1 antibodies (pcPREL1) as indicated. (c) Pull-down experiments of Ena/VASP proteins using the GST-tagged proline rich N- (PR-N) or C-terminus (PR-C) of PREL1. Lysates from Rat2 cells expressing endogenous Mena and from NIH3T3 cells expressing high levels of endogenous VASP were challenged with the immobilized GST-tagged proline rich N- or C-terminus of PREL1. Western blot detection was performed using either a monoclonal anti-Mena antibody [21] or polyclonal anti-VASP antibodies (pcVASP). Endogenous VASP and Mena were readily co-precipitated. (d) Control pull-down experiments using immobilized GST alone from lysates of NIH 3T3 cells transfected with different GFP-tagged PREL1 constructs. Cell lysates (1) were loaded next to the GST pulldowns (2) and Western blot detection was performed using the monoclonal anti GFP antibody. Note that GST does not co-precipitate the GFP-PREL1 or truncated mutants. (e,f) Peptide overlays of the proline-rich N-terminus (e) or C-terminus (f) of PREL1 with the GST-tagged EVH1 domain of Mena. Boxes and arrows depict the amino acid sequences of the spots showing the strongest signals within the N- or C-terminus of PREL1 as indicated.

3.4. Interaction of PREL1 with phosphoinositides and Ras-GTPases

The central region of PREL1 comprises a RA and a PH domain embedded within the GM region of homology (see also Fig. 1(c)). A common feature of PH domains, which occur in a wide range of proteins, is their ability to bind inositol phosphates and to be targeted to membranous compartments [48]. In order to test for potential phospholipid binding of the PREL1-PH domain, we overlayed a membrane with immobilized phospho-lipids (PIP Strip, Echelon Research Inc.) with the recombinant GST-tagged PH domain of PREL1, in analogy to the peptide overlay technique.

Excitingly, the PH domain of PREL1 displayed highest binding affinity to phosphatidylinositol monophosphates PtdIns(5)P and PtdIns(3)P (Fig. 4(a)), which reflects the binding characteristics shown for the same domain in Grb7 [49]. Binding of the GST-tagged PH domain to immobilized lipids was quantified luminometrically and revealed signals for PtdIns(5)P > PtdIns(3)P > PtdIns of 100, 65.8 and 47.6 (arbitrary units), respectively.

We then tested whether the RA domain of PREL1 might bind to Ras-family GTPases. RA domains have been identified in RasGTP effector proteins such as RalGDS [50,51]. Some downstream effectors of Ras GTPases, such as Nore1/RapL, have the ability to bind to GTP loaded H-, K- and N-Ras as well as to Rap1 via their RA domain and to act in a cell type specific manner [52,53]. Interestingly, the highly similar RA domains of Grb7/10/14 proteins were not found to bind to RasGTP [54,55]. Very recently, however, full length Grb7 as well as a N-terminal fragment of the human ortholog of PREL1, which includes the RA but not the PH domain, was reported to bind to Ras in pull-down assays [56]. To test for the Ras-binding capabilities of the RA domain of PREL1, we first performed pull-down assays from lysates of cells expressing constitutively active mutants of various Ras superfamily GTPases using the recombinant GST-tagged RA domain of PREL1. Under these conditions, GST-RA of PREL1 co-precipitated only low amounts of H-RasV12 (Fig. 4(b)) and K-RasV12 (not shown).

To test whether PREL1 can associate with members of the Ras family of GTPases in vivo, we performed co-immunoprecipitations of endogenous PREL1 with ectopically expressed myc-tagged constitutively activated mutants of Ras, Rap1, Rac1, Cdc42 or RhoA using the polyclonal anti-PREL1 antiserum. Notably, full length PREL1 could co-immunoprecipitate significant amounts of RasV12 (Fig. 4(c)), but only in the complete absence of detergents, while even low amounts of Triton-X100 or NP-40 completely abolished this interaction (Fig. 4(c), lower panel). Members of the Rho family did not co-precipitate with PREL1 (not shown), and even the Ras-family GTPase Rap1 was not detectable in immunoprecipitates of PREL1 under these conditions (Fig. 4(c)), indicating that binding of PREL1 to small GTPases may be highly specific also within the Ras-subfamily. Together, these findings indicate that binding of PREL1 to Triton-soluble components, such as most phospholipids, is required for efficient binding of the RA domain to activated Ras-GTPases.

From these data, we hypothesize that membrane binding of the PH domain might cooperate with the RA domain to associate with RasGTP during signal transmission. Moreover, a potential dependency of RA domain binding to RasGTP on the presence of an intact PH domain and phosphoinositides might well explain results from an earlier study, in which RA-domains of the Grb-family were reported not to bind Ras GTP-ases [37,54]. This view is not only supported by the high sequence conservation of the RA-PH domain tandem between PREL1/2 and the Grb7/10/14 proteins, but also by the striking similarity in PtdIns phosphate binding characteristics of the isolated PH domains of both sub-families. In the light of these findings, it will be interesting to re-evaluate the GTPase binding characteristics of all Grb7/10/14 family members. Finally, in an independent study, Lafuente and colleagues have now described the human ortholog of murine PREL1 as an interactor of Rap1 in Jurkat T-cells and termed this protein RIAM (for Rap interacting adaptor molecule) [57]. In yeast two-hybrid assays, these authors also detected an interaction with H-Ras, albeit weaker than that with Rap1. Resolving the discrepancies between the observations from the latter and the present study requires further investigations.

3.5. Localization of PREL1 coincides with Ras activation in NIH3T3 cells

Due to the ability of PREL1 to bind to RasGTP, we asked as to whether its localization or recruitment might be regulated

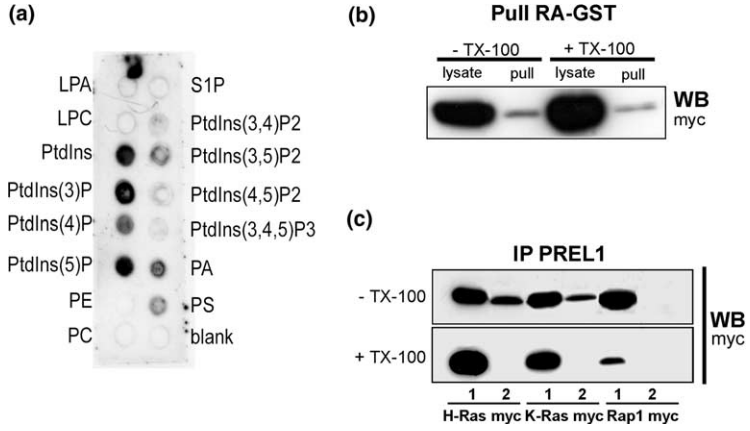

Fig. 4. PREL1 binds to constitutively active Ras in a lipid-dependent manner. (a) A PIP-strip was overlayed with the PH domain of PREL1 fused to GST. Detection of bound protein was performed using a monoclonal anti-GST antibody followed by peroxidase-coupled secondary reagents and chemiluminescence. The signal was detected and quantified using a CCD camera (see text for further details). Strong binding was detected for phosphatidyl monophosphates (PtdIns(3)P and PtdIns(5)P) and, albeit weaker, for phosphatidyl inositide (PtdIns). (b) Pull-down experiments using the recombinant GST-tagged RA domain of PREL1 performed on lysates of NIH3T3 cells expressing myc-tagged RasV12, lysed in the presence and absence of Triton X-100 (TX-100). (c) Co-immunoprecipitations of PREL1 and Ras-family GTPases from lysates of NIH3T3 cells expressing constitutively active versions of H-Ras, K-Ras and Rap1. Immunoprecipitations using the polyclonal anti PREL1 antibody pcPREL1 revealed a specific binding of PREL1 to Ras, but not Rap1 (upper panel). Binding of Ras GTPases to endogenous full length PREL1 was completely abolished in the presence of Triton-X 100 (lower panel). Lanes corresponding to cell lysates (relative loading 1/10) and immunoprecipitates are labelled with 1 and 2, respectively.

by cellular RasGTP levels. This possibility seemed attractive, since it might explain for the differences in subcellular recruitment under different conditions and in different cell types (also compare to Fig. 2).

It was previously shown that spreading of NIH3T3 cells on fibronectin coincides with increased Ras activity, reaching a maximum in the first 10 min and then declining to basal levels within 60 min [58]. Under these conditions, Ras activation was also reported to be accompanied by Erk (extracellular signal regulated kinase) activation [58]. Moreover, Nobes and Hall reported that Ras- and Erk activation during cell migration, induced by wounding of cell monolayers, is required for efficient translocation of the cells into the wound [2].

To learn more about the recruitment mechanisms of PREL1, we studied the subcellular distribution of PREL1 in NIH3T3 cells during spreading on fibronectin in the context of cellular RasGTP levels, as determined by Ras activation assays. The time course of Ras activation in NIH3T3 cells is shown in Fig. 5(a) and is virtually identical to the results obtained in earlier studies [58]. Intriguingly, microscopic analysis of cells, processed in parallel in order to study the subcellular distribution of endogenous PREL1, revealed a clear recruitment of PREL1 to the tips of circular lamellipodia typically occurring during cell spreading on fibronectin (Fig. 5(b)). To assess if the number of cells displaying lamellipodial recruitment of PREL1 correlates with the levels of cellular Ras-activation, we performed detailed quantifications of the percentage of cells that are spread at a given timepoint (line plot in Fig. 5(c)) as compared to the percentage of spread cells that display lamellipodial tip localization of PREL1 (column plot in Fig. 5(c)). A clear correlation of high Ras activity and PREL1 localization during spreading could be observed. After 60 min, when cellular Ras-GTP levels had returned to a basal level, cells displaying lamellipodial PREL1 localization were observed only rarely, while Ena/VASP proteins still displayed the typical subcellular distribution (lower left image in Fig. 5(b)) described in earlier studies [9,20]. Hence, we conclude that PREL1 is not essential for the constitutive recruitment of Ena/VASP proteins to lamellipodia or focal adhesions, but instead is recruited to the sites of rapid actin turnover during Ras activation, where it may then modulate actin assembly by interaction with Ena/VASP proteins.

To further corroborate the coincidence between Ras activation and the translocation of PREL1 to sites of cellular actin assembly, such as lamellipodia and focal adhesions, we experimentally increased Ras activity in these cells by either microinjection of constitutively active recombinant RasV12 (Fig. 6(a)) or by TPA treatment (Fig. 6(b)), which was described earlier to significantly increase Ras-GTP levels in NIH3T3 cells [59]. In response to both treatments, PREL1 was clearly recruited to focal adhesions, confirming that PREL1 indeed associates with the actin cytoskeleton in response to Ras activation.

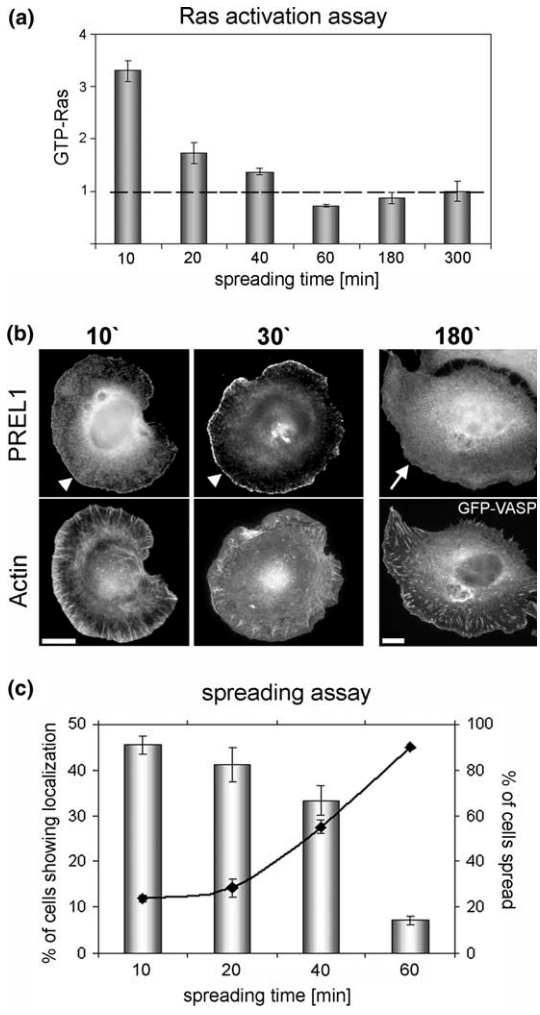

Fig. 5. Actin cytoskeletal targeting of PREL1 correlates with Ras activation during cell spreading. (a) Ras activity in spreading NIH 3T3 fibroblasts was quantified at different timepoints after plating on fibronectin as indicated, employing a Ras activation assay based on Ras-GTP pulldowns using the GST-tagged Ras binding domain (RBD) of Raf1. (b) Localization of PREL1 during spreading on fibronectin was determined by indirect immunofluorescence at different timepoints after plating on fibronectin-coated coverslips using polyclonal anti PREL1 antibodies (pcPREL1). Note that the recruitment of PREL1 to lamellipodia is largely lost at late stages of spreading (upper right image), while VASP remained prominently associated with lamellipodia and focal adhesions (lower right image). Scale bars equal 10 μm. (c) Quantification of the percentage of spread cells at the timepoints indicated (line plot) as compared to the percentage of spread cells displaying lamellipodial tip localization (column plot). Values are means ± standard errors of means from three independent experiments ($n \geqslant 300$ for each condition).

4. Conclusions

We here report the identification and characterization of a novel proline rich protein, capable of interacting with the Ena/VASP family of proteins and of targeting to lamellipodia tips and focal adhesions coincident with high RasGTP levels. We map in detail the binding sites of the EVH1 domains of Ena/VASP proteins on the proline rich N- and C-termini of PREL1, in addition to characterizing the binding features of its central RA - and PH domain. We show that PREL1 specifically associates with Ras via its RA domain in a lipid dependent fashion, the latter of which is most likely attributable to the adjacent PH domain. Finally, we demonstrate that the subcellular targeting of PREL1 to lamellipodia and focal adhesions correlates with high Ras-GTP levels as induced for instance during cell spreading or by phorbol ester treatment.

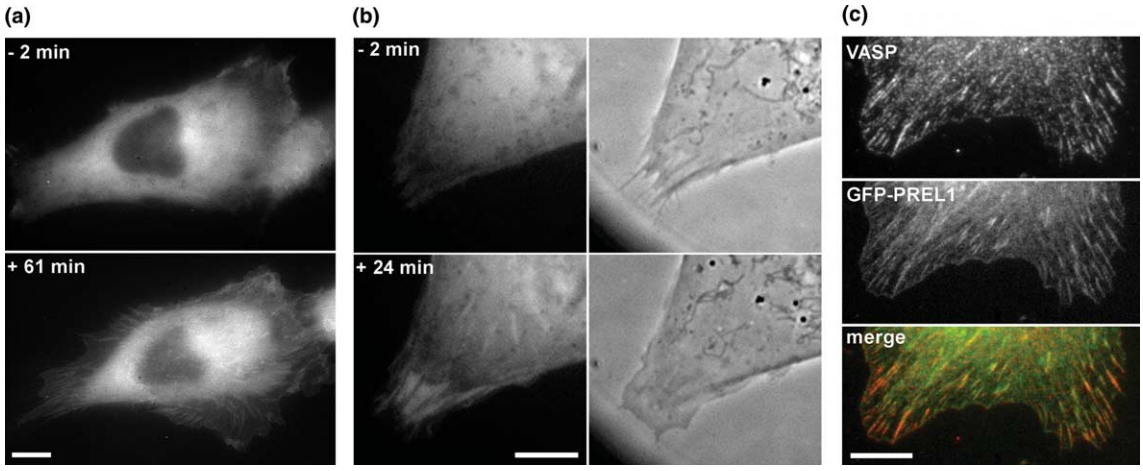

Fig. 6. Translocation of PREL1 upon experimentally induced Ras activation. (a,b) Time lapse fluorescence and phase contrast microscopy of NIH 3T3 fibroblasts transfected with GFP-tagged full length PREL1 before (−2 min) and after (+61 min) microinjection of constitutively active Ras V12 (a) or before (−2 min) and after (+24 min) treatment with the phorbol ester TPA (b). Significant translocation of largely cytosolic GFP-PREL1 to focal adhesions upon experimentally induced increase in cellular Ras-GTP levels could be observed. (c) NIH 3T3 cells expressing GFP-tagged PREL1 (green in merge) and counterstained for endogenous VASP (red in merge) as indicated following TPA treatment (15 min). Note the colocalization of PREL1 and VASP under these conditions. Scale bars equal 10 μm.

Together, these data suggest that the novel Ena/VASP interactor PREL1 functions in the signal transduction from Ras activation to actin cytoskeletal remodelling.

Acknowledgement: We thank Petra Hagendorff for excellent technical assistance and Marlies Konradt for expert help with antibody generation. We are grateful to Gabriele Mayr and Dr. Matthias Krause for collaborating in the initial 31C4 screen and Dr. Klemens Rottner for performing microinjections and critically reading the manuscript. We thank Drs. Ronald Frank and Werner Tegge for generously providing peptide scans and peptides for immunization. This work was supported in part by the DFG (666/1-1 to T.E.B.S. and J.W.), the Fonds der Chemischen Industrie (to J.W.) and by a grant from the Austrian Science Research Council, P14660-PAT (to J.V.S.).

Appendix A. Supplementary data

Supplementary data associated with this article can be found, in the online version, at doi:10.1016/j.febslet.2004.10.110.

References

[1] Nobes, C. and Hall, A. (1994) Regulation and function of the Rho subfamily of small GTPases. Curr. Opin. Genet. Dev. 4, 77–81.
[2] Nobes, C.D. and Hall, A. (1999) Rho GTPases control polarity, protrusion, and adhesion during cell movement. J. Cell Biol. 144, 1235–1244.
[3] Pollard, T.D. and Borisy, G.G. (2003) Cellular motility driven by assembly and disassembly of actin filaments. Cell 112, 453–465.
[4] Pantaloni, D., Le Clainche, C. and Carlier, M.F. (2001) Mechanism of actin-based motility. Science 292, 1502–1506.
[5] Wang, Y.L. (1985) Exchange of actin subunits at the leading edge of living fibroblasts: possible role of treadmilling. J. Cell Biol. 101, 597–602.
[6] Small, J.V., Isenberg, G. and Celis, J.E. (1978) Polarity of actin at the leading edge of cultured cells. Nature 272, 638–639.
[7] Steffen, A., Rottner, K., Ehinger, J., Innocenti, M., Scita, G., Wehland, J. and Stradal, T.E. (2004) Sra-1 and Nap1 link Rac to actin assembly driving lamellipodia formation. Embo J. 23, 749–759.
[8] Innocenti, M., et al. (2004) Abi1 is essential for the formation and activation of a WAVE2 signalling complex. Nat. Cell Biol. 6, 319–327.
[9] Rottner, K., Behrendt, B., Small, J.V. and Wehland, J. (1999) VASP dynamics during lamellipodia protrusion. Nat. Cell Biol. 1, 321–322.
[10] Small, J.V., Stradal, T., Vignal, E. and Rottner, K. (2002) The lamellipodium: where motility begins. Trends Cell Biol. 12, 112–120.
[11] Bear, J.E., Loureiro, J.J., Libova, I., Fassler, R., Wehland, J. and Gertler, F.B. (2000) Negative regulation of fibroblast motility by Ena/VASP proteins. Cell 101, 717–728.
[12] Bear, J.E., et al. (2002) Antagonism between Ena/VASP proteins and actin filament capping regulates fibroblast motility. Cell 109, 509–521.
[13] Bar-Sagi, D. and Feramisco, J.R. (1986) Induction of membrane ruffling and fluid-phase pinocytosis in quiescent fibroblasts by ras proteins. Science 233, 1061–1068.
[14] Hughes, P.E., Renshaw, M.W., Pfaff, M., Forsyth, J., Keivens, V.M., Schwartz, M.A. and Ginsberg, M.H. (1997) Suppression of integrin activation: a novel function of a Ras/Raf-initiated MAP kinase pathway. Cell 88, 521–530.
[15] Kinbara, K., Goldfinger, L.E., Hansen, M., Chou, F.L. and Ginsberg, M.H. (2003) Ras GTPases: integrins' friends or foes?. Nat. Rev. Mol. Cell Biol. 4, 767–776.
[16] Kitayama, H., Sugimoto, Y., Matsuzaki, T., Ikawa, Y. and Noda, M. (1989) A ras-related gene with transformation suppressor activity. Cell 56, 77–84.
[17] Bos, J.L., et al. (2003) The role of Rap1 in integrin-mediated cell adhesion. Biochem. Soc. Trans. 31, 83–86.
[18] Miyamoto, S., Teramoto, H., Coso, O.A., Gutkind, J.S., Burbelo, P.D., Akiyama, S.K. and Yamada, K.M. (1995) Integrin function: molecular hierarchies of cytoskeletal and signaling molecules. J. Cell Biol. 131, 791–805.
[19] Samarin, S., Romero, S., Kocks, C., Didry, D., Pantaloni, D. and Carlier, M.F. (2003) How VASP enhances actin-based motility. J. Cell Biol. 163, 131–142.
[20] Reinhard, M., Halbrugge, M., Scheer, U., Wiegand, C., Jockusch, B.M. and Walter, U. (1992) The 46/50 kDa phosphoprotein VASP purified from human platelets is a novel protein associated with actin filaments and focal contacts. Embo J. 11, 2063–2070.
[21] Gertler, F.B., Niebuhr, K., Reinhard, M., Wehland, J. and Soriano, P. (1996) Mena, a relative of VASP and Drosophila Enabled, is implicated in the control of microfilament dynamics. Cell 87, 227–239.

[22] Svitkina, T.M., Bulanova, E.A., Chaga, O.Y., Vignjevic, D.M., Kojima, S., Vasiliev, J.M. and Borisy, G.G. (2003) Mechanism of filopodia initiation by reorganization of a dendritic network. J. Cell Biol. 160, 409–421.
[23] Reinhard, M., Giehl, K., Abel, K., Haffner, C., Jarchau, T., Hoppe, V., Jockusch, B.M. and Walter, U. (1995) The proline-rich focal adhesion and microfilament protein VASP is a ligand for profilins. Embo J. 14, 1583–1589.
[24] Geese, M., Loureiro, J.J., Bear, J.E., Wehland, J., Gertler, F.B. and Sechi, A.S. (2002) Contribution of Ena/VASP proteins to intracellular motility of listeria requires phosphorylation and proline-rich core but not F-actin binding or multimerization. Mol. Biol. Cell 13, 2383–2396.
[25] Loisel, T.P., Boujemaa, R., Pantaloni, D. and Carlier, M.F. (1999) Reconstitution of actin-based motility of Listeria and Shigella using pure proteins. Nature 401, 613–616.
[26] Grenklo, S., Geese, M., Lindberg, U., Wehland, J., Karlsson, R. and Sechi, A.S. (2003) A crucial role for profilin-actin in the intracellular motility of Listeria monocytogenes. EMBO Rep. 4, 523–529.
[27] Frischknecht, F. and Way, M. (2001) Surfing pathogens and the lessons learned for actin polymerization. Trends Cell Biol. 11, 30–38.
[28] Niebuhr, K., et al. (1997) A novel proline-rich motif present in ActA of Listeria monocytogenes and cytoskeletal proteins is the ligand for the EVH1 domain, a protein module present in the Ena/VASP family. Embo J. 16, 5433–5444.
[29] Reinhard, M., Jouvenal, K., Tripier, D. and Walter, U. (1995) Identification, purification, and characterization of a zyxin-related protein that binds the focal adhesion and microfilament protein VASP (vasodilator-stimulated phosphoprotein). Proc. Natl. Acad. Sci. USA 92, 7956–7960.
[30] Reinhard, M., Rudiger, M., Jockusch, B.M. and Walter, U. (1996) VASP interaction with vinculin: a recurring theme of interactions with proline-rich motifs. FEBS Lett. 399, 103–107.
[31] Krause, M., Sechi, A.S., Konradt, M., Monner, D., Gertler, F.B. and Wehland, J. (2000) Fyn-binding protein (Fyb)/SLP-76-associated protein (SLAP), Ena/vasodilator-stimulated phosphoprotein (VASP) proteins and the Arp2/3 complex link T cell receptor (TCR) signaling to the actin cytoskeleton. J. Cell Biol. 149, 181–194.
[32] Boukhelifa, M., Parast, M.M., Bear, J.E., Gertler, F.B. and Otey, C.A. (2004) Palladin is a novel binding partner for Ena/VASP family members. Cell Motil Cytoskeleton 58, 17–29.
[33] Tanoue, T. and Takeichi, M. (2004) Mammalian Fat1 cadherin regulates actin dynamics and cell–cell contact. J. Cell Biol. 165, 517–528.
[34] Rottner, K., Krause, M., Gimona, M., Small, J.V. and Wehland, J. (2001) Zyxin is not colocalized with vasodilator-stimulated phosphoprotein (VASP) at lamellipodial tips and exhibits different dynamics to vinculin, paxillin, and VASP in focal adhesions. Mol. Biol. Cell 12, 3103–3113.
[35] Manser, J. and Wood, W.B. (1990) Mutations affecting embryonic cell migrations in *Caenorhabditis elegans*. Dev. Genet. 11, 49–64.
[36] Manser, J., Roonprapunt, C. and Margolis, B. (1997) C. elegans cell migration gene mig-10 shares similarities with a family of SH2 domain proteins and acts cell nonautonomously in excretory canal development. Dev. Biol. 184, 150–164.
[37] Han, D.C., Shen, T.L. and Guan, J.L. (2001) The Grb7 family proteins: structure, interactions with other signaling molecules and potential cellular functions. Oncogene 20, 6315–6321.
[38] Daly, R.J. (1998) The Grb7 family of signalling proteins. Cell Signal 10, 613–618.
[39] Ballestrem, C., Wehrle-Haller, B. and Imhof, B.A. (1998) Actin dynamics in living mammalian cells. J. Cell Sci. 111 (Pt 12), 1649–1658.
[40] Niebuhr, K., Lingnau, A., Frank, R. and Wehland, J. (1998) Rapid procedures for preparing monoclonal antibodies and identifying their epitopesCell Biology: A Laboratory Handbook, vol. 2, pp. 398–403, Academic Press, San Diego.
[41] Mies, B., Rottner, K. and Small, J.V. (1997) Immunofluorescence microscopy of the cytoskeleton: Double and triple immunofluorescence II (Celis, J.E., Ed.), Cell Biology: A Laboratory Handbook, vol. 2, pp. 469–476, Academic Press, London.
[42] Ridley, A.J. and Hall, A. (1992) The small GTP-binding protein rho regulates the assembly of focal adhesions and actin stress fibers in response to growth factors. Cell 70, 389–399.
[43] Carl, U.D., Pollmann, M., Orr, E., Gertlere, F.B., Chakraborty, T. and Wehland, J. (1999) Aromatic and basic residues within the EVH1 domain of VASP specify its interaction with proline-rich ligands. Curr. Biol. 9, 715–718.
[44] Ermekova, K.S., Zambrano, N., Linn, H., Minopoli, G., Gertler, F., Russo, T. and Sudol, M. (1997) The WW domain of neural protein FE65 interacts with proline-rich motifs in Mena, the mammalian homolog of Drosophila enabled. J. Biol. Chem. 272, 32869–32877.
[45] Forrester, W.C., Perens, E., Zallen, J.A. and Garriga, G. (1998) Identification of *Caenorhabditis elegans* genes required for neuronal differentiation and migration. Genetics 148, 151–165.
[46] Hadano, S., et al. (2001) A gene encoding a putative GTPase regulator is mutated in familial amyotrophic lateral sclerosis 2. Nat. Genet. 29, 166–173.
[47] Frank, R. (2002) The SPOT-synthesis technique. Synthetic peptide arrays on membrane supports – principles and applications. J. Immunol. Methods 267, 13–26.
[48] Lemmon, M.A. (2003) Phosphoinositide recognition domains. Traffic 4, 201–213.
[49] Shen, T.L., Han, D.C. and Guan, J.L. (2002) Association of Grb7 with phosphoinositides and its role in the regulation of cell migration. J. Biol. Chem. 277, 29069–29077.
[50] Vetter, I.R., Linnemann, T., Wohlgemuth, S., Geyer, M., Kalbitzer, H.R., Herrmann, C. and Wittinghofer, A. (1999) Structural and biochemical analysis of Ras-effector signaling via RalGDS. FEBS Lett. 451, 175–180.
[51] Wojcik, J., Girault, J.A., Labesse, G., Chomilier, J., Mornon, J.P. and Callebaut, I. (1999) Sequence analysis identifies a ras-associating (RA)-like domain in the N-termini of band 4.1/JEF domains and in the Grb7/10/14 adapter family. Biochem. Biophys. Res. Commun. 259, 113–120.
[52] Katagiri, K., Maeda, A., Shimonaka, M. and Kinashi, T. (2003) RAPL, a Rap1-binding molecule that mediates Rap1-induced adhesion through spatial regulation of LFA-1. Nat. Immunol. 4, 741–748.
[53] Oertli, B., Han, J., Marte, B.M., Sethi, T., Downward, J., Ginsberg, M. and Hughes, P.E. (2000) The effector loop and prenylation site of R-Ras are involved in the regulation of integrin function. Oncogene 19, 4961–4969.
[54] Leavey, S.F., Arend, L.J., Dare, H., Dressler, G.R., Briggs, J.P. and Margolis, B.L. (1998) Expression of Grb7 growth factor receptor signaling protein in kidney development and in adult kidney. Am. J. Physiol. 275, F770–F776.
[55] Riedel, H. (2004) Grb10 exceeding the boundaries of a common signaling adapter. Front Biosci. 9, 603–618.
[56] Rodriguez-Viciana, P., Sabatier, C. and McCormick, F. (2004) Signaling specificity by Ras family GTPases is determined by the full spectrum of effectors they regulate. Mol. Cell Biol. 24, 4943–4954.
[57] Lafuente, E.M., et al. (2004) RIAM, an Ena/VASP and profilin ligand, interacts with Rap1-GTP and mediates Rap1-induced adhesion. Dev. Cell 7, 585–595.
[58] Clark, E.A. and Hynes, R.O. (1996) Ras activation is necessary for integrin-mediated activation of extracellular signal-regulated kinase 2 and cytosolic phospholipase A2 but not for cytoskeletal organization. J. Biol. Chem. 271, 14814–14818.
[59] El-Shemerly, M.Y.M., Besser, D., Nagasawa, M. and Nagamine, Y. (1997) 12-O-tetradecanoylphorbol-13acetate activates the Ras/extracellular signal-regulated kinase (ERK) signaling pathway upstream of SOS involving serine phosphorylation of Shc in NIH3T3 cells. J. Biol. Chem. 272, 30599–30602.